



## The year in cardiology 2019

# The year in cardiology: imaging

Dudley Pennell<sup>1</sup>, Victoria Delgado<sup>2</sup>, Juhani Knuuti<sup>3</sup>, Pål Maurovich-Horvat<sup>4</sup>, and Jeroen J. Bax<sup>2\*</sup>

<sup>1</sup>Cardiovascular Magnetic Resonance Unit, Royal Brompton Hospital, National Heart and Lung Institute, Imperial College, London, UK; <sup>2</sup>Department of Cardiology, Heart LungCentre, Leiden University Medical Centre, Leiden, The Netherlands; <sup>3</sup>Turku PET Centre, University of Turku, and Turku University Hospital, Turku, Finland; and <sup>4</sup>MTA-SE Cardiovascular Imaging Research Group, Heart and Vascular Centre, Semmelweis University, Budapest, Hungary

Received 11 November 2019; revised 28 November 2019; editorial decision 10 December 2019; accepted 11 December 2019

Ovaj rad je preuzet sa odobrenjem u okviru Editors Network pod okriljem ESC.

This paper has been reproduced with permission through Editors network under auspices of ESC.

## Introduction

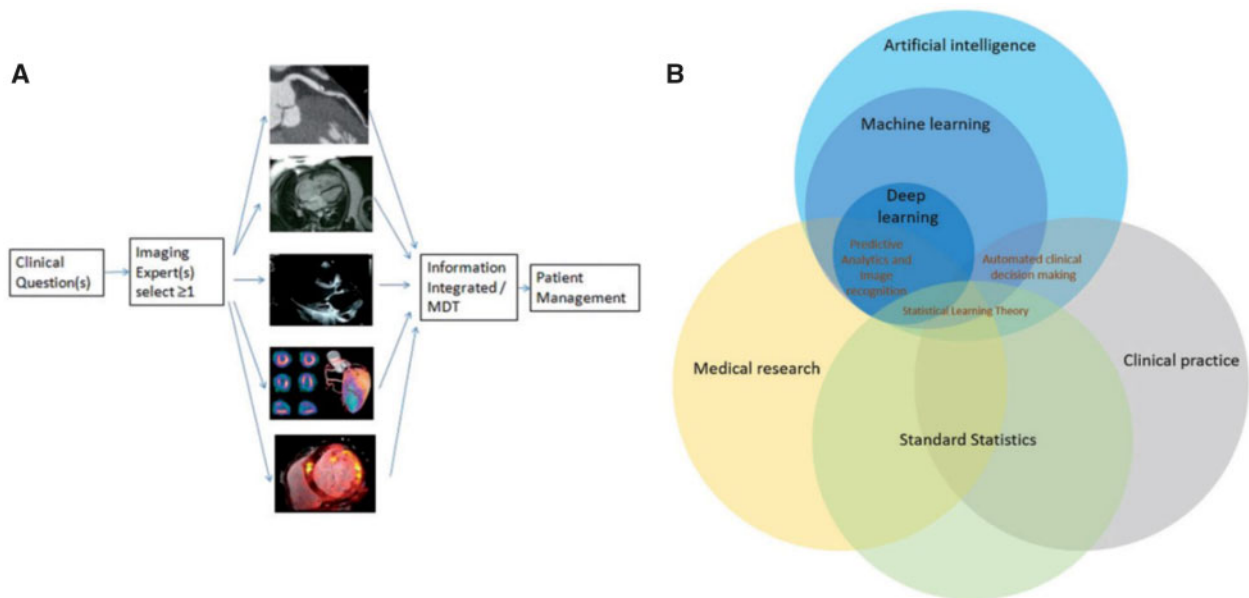
**M**ultimodality imaging and artificial intelligence applied to imaging techniques have been a major interest in this year. The pathophysiological insights that various imaging modalities have provided in numerous clinical scenarios (heart failure, coronary artery disease, and valvular heart disease) influence the way we evaluate and manage patients. Conventional imaging to assess cardiac structure and function is still the first approach to evaluate patients and decide the management. However, advanced echocardiography with strain imaging techniques, tissue characterization with cardiovascular magnetic resonance (CMR), and assessment of biological processes with nuclear imaging techniques have helped to understand that early intervention may be needed in order to prevent or halt the progression of the disease. By applying machine learning techniques to all these imaging modalities, we are able to generate algorithms that can identify certain patterns of disease or risk and develop decisions in a more personalized way. This Year in Cardiology review articles summarize the most relevant studies in the field of imaging published in the last year.

This year, artificial intelligence and machine learning applied to cardiac imaging has been one of the main novelties. Other advances in non-invasive cardiac imaging published in 2019 are summarized in this Year in Cardiology review article (*Take home figure*).

## Echocardiography

Early detection of left ventricular (LV) dysfunction in various populations has been the focus of numerous publications in 2019. Left ventricular diastolic function usually precedes LV systolic dysfunction and is associated with cardiovascular morbidity and mortality. From the Copen-

hagen City Heart Study, a population-based study including 6238 individuals, Lassen *et al.*<sup>3</sup> evaluated the association between LV filling pressures measured on tissue Doppler imaging ( $E/E^0$ ) and speckle tracking echocardiography ( $E/E^{0sr}$ ) with the occurrence of cardiovascular death, admission for incident heart failure or myocardial infarction (MI). Of 1238 participants, 140 (11.3%) reached the primary endpoint during a median follow-up of 11 years. After adjusting for various clinical and echocardiographic parameters,  $E/E^{0sr}$  was independently associated with the endpoint [hazard ratio (HR) 1.08, 95% confidence interval (CI) 1.02–1.13 per each 10 cm increase;  $P = 0.003$ ] whereas  $E/E^0$  was not. In addition,  $E/E^{0sr}$  provided incremental prognostic value over the SCORE risk chart, currently used to evaluate the risk of cardiovascular morbidity and mortality in the general population. Increased LV filling pressures may reflect the ageing process of the heart characterized by increased fibrosis. This fibrosis may lead to conduction abnormalities that influence the contractile function of the LV. Modin *et al.*<sup>4</sup> evaluated in 1138 participants of the Copenhagen City Heart Study the prognostic value of LV mechanical dispersion which is measured as the standard deviation from time to peak longitudinal strain of the three LV apical views. The mean value of LV mechanical dispersion in the general population was  $45 \pm 38$  ms and increased with age, hypertension, body mass index, and presence of MI. Large LV mechanical dispersion was associated with worse LV systolic and diastolic function. Each 10 ms increase in LV mechanical dispersion was independently associated with increased risk of cardiovascular death (HR 1.04, 95% CI 1.01–1.06;  $P = 0.004$ ). Despite the growing evidence on the diagnostic and prognostic value of strain derived measures of LV systolic and diastolic function, LV ejection fraction (EF) remains the mainstay parameter for risk stratification in clinical practice. The association between physician reported LVEF and sur-



**Take home figure** Multimodality imaging and artificial intelligence in cardiac imaging. The use of the different imaging modalities should be based on a clinical question. Selecting the most appropriate imaging techniques and integrate them to answer that specific question will be key to improve the outcomes of patients (A). In the future, many of the process the clinicians are used to do to integrate all the information gathered from the imaging modalities may be automated by using artificial intelligence techniques. How artificial intelligence interacts with medical research, clinical practice and statistics will be the focus of ongoing research (B). Reproduced with permission from Fox et al.<sup>1</sup> and Krittanawong et al.<sup>2</sup>

vival was assessed in 403 977 echocardiograms performed in 203 135 patients from USA.<sup>5</sup> Fifty percent of the population had an LVEF between 55% and 65%. Over a median follow-up of 4 years, 23% of patients died. A U-shaped relationship between LVEF and all-cause mortality was observed with the nadir at the 60–65% LVEF category. These results were reproduced in an independent dataset from New Zealand including 45 531 echocardiograms from 35 976 patients. The U-shaped relationship was also observed in men and women, inpatients and outpatients with heart failure, and deviations from LVEF of 60–65% were associated with greater multiplicative increase in risk for younger patients as compared to old patients.

Left ventricular ejection fraction is also the parameter to classify heart failure patients. Ten to 20% of patients with heart failure with reduced LVEF ( $\leq 40\%$ ) may improve in LVEF. However, the evidence on the frequency and outcomes of patients with heart failure and recovered LVEF is based on selected cohort of patients or randomized clinical trials. Of 3124 heart failure patients with reduced LVEF at baseline treated with contemporary heart failure medications, 37.6% presented improvement in LVEF from 26% to 46% over a median follow-up of 17 months.<sup>6</sup> Patients with heart failure and recovered LVEF had lower rates for all-cause mortality, all-cause hospitalizations, cardiac transplantation, or LV assist device implantation than the patients who remained with reduced LVEF. Not less important is the characterization of the right ventricular (RV) remodelling in heart failure patients. In 271 patients with heart failure and preserved LVEF (HFpEF), RV fractional area change reduced by 10% and RV diastolic area increased by 21% over a median follow-up of 4 years.<sup>7</sup> These changes exceeded the corresponding changes in

the LV. In addition, the prevalence of tricuspid regurgitation increased by 45%. Atrial fibrillation, higher body weight, coronary artery disease, higher pulmonary pressures and LV filling pressures and RV dilation were associated with development of RV dysfunction (*Figure 1*).<sup>7</sup> Patients with HFpEF developing RV dysfunction had two-fold increased risk of death. In this group of heart failure patients, assessment of left atrial function has provided important new insights. In 308 patients with HFpEF, Freed *et al.*<sup>8</sup> showed that impaired left atrial reservoir strain (stiff left atrium) was associated with increased pulmonary vascular resistance and decreased peak oxygen consumption and was independently associated with the composite outcome of cardiovascular hospitalization or death. It should be noted that the study did not correct the association between left atrial reservoir strain and the composite outcome for neuro-hormonal markers and as acknowledged by the authors, the studies establishing the reference values of normal left atrial strain values across the echocardiographic systems and analysis platforms are scarce.

In patients with asymptomatic severe aortic stenosis and preserved LVEF, LV global longitudinal strain (GLS) on speckle tracking echocardiography is more sensitive than LVEF to identify early changes in LV systolic function during the follow-up. An LV GLS of  $> -18.2\%$  (more impaired) is associated with higher risk of developing symptoms and needing aortic valve intervention as compared to more preserved values of LV GLS ( $\leq -18.2\%$ ).<sup>9</sup> Echocardiography is the imaging technique of first choice to assess valvular heart disease. Secondary mitral regurgitation quantification remains challenging. In 423 heart failure patients, Bartko *et al.*<sup>10</sup> developed a unifying algorithm combining effective regurgitant orifice area (EROA), regurgitant volume, and regurgitant fraction that had better discrimina-

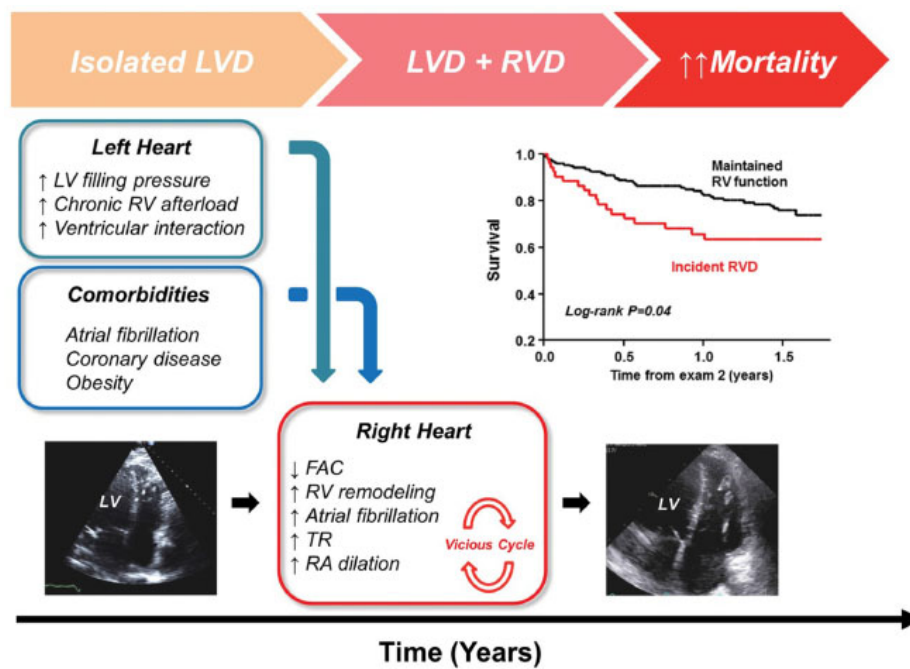


**Figure 1** Development of right ventricular dysfunction (RVD) over time in patients with heart failure and preserved ejection fraction. Increased left ventricular (LV) filling pressures and associated comorbidities characterize the initial phase of isolated left ventricular dysfunction (LVD) and lead to right ventricular (RV) remodelling, right ventricular dysfunction. Patients with incident right ventricular dysfunction have worse outcome as compared to patients with preserved RV function. Reproduced with permission from Obokata et al.<sup>7</sup>

tionpower to identify patients with increased mortality risk than current guideline-based definitions. Low-risk patients were characterized by an EROA of  $<20 \text{ mm}^2$  and a regurgitant volume of  $<30 \text{ mL}$  whereas high-risk patients were defined by an EROA of  $\geq 30 \text{ mm}^2$  and a regurgitant volume of  $\geq 45 \text{ mL}$ . Intermediate-risk patients (with an EROA between 20 and 29  $\text{mm}^2$  and a regurgitant volume of 30–44 mL) were reclassified as high risk if the regurgitant fraction was  $\geq 50\%$ . However, this algorithm had a rather modest discrimination power (area under the curve 0.63).

The use of transthoracic focused cardiac ultrasound (FoCUS) is gaining popularity at the emergency department and intensive care units. Among 839 patients with suspected acute aortic syndrome, an aortic dissection detection risk score of  $\leq 1$  and a negative FoCUS could rule out an acute aortic syndrome with a sensitivity of 94% and a failure rate of 1.9%.<sup>11</sup>

Finally, elevated carotid artery wave intensity measured on Duplex Doppler ultrasound was independently associated with faster cognitive decline among 3191 individuals enrolled in the Whitehall II study,<sup>12</sup> highlighting the relevance of ultrasound imaging outside the heart.

## Cardiovascular magnetic resonance

The ICELAND-MI study is providing significant new data in the understanding of MI and fibrosis in elderly adults. In the first report by Shanbhag et al.,<sup>13</sup> 397 patients aged 72–81 years were studied using CMR incorporating late gadolinium enhancement (LGE) imaging which identifies myocardial fibrosis due to MI (subendocardial) and other causes (other patterns). During the follow-up of 5.8 years,

192 events were recorded. The authors found that major non-ischaemic fibrosis was the only independent predictor of outcome (Figure 2).<sup>13</sup>

In the second report from the ICELAND-MI trial, Acharya et al.<sup>14</sup> report on the long-term predictive value of unrecognized MI (UMI) in an elderly cohort of 935 subjects aged 67–93 years. Previous reports have suggested a poor short-term prognosis but this study extends follow-up to 13.3 years. The authors showed that all-cause mortality in UMI patients was lower than recognized MI for at least 5 years, but similar at 10 years. At all time-points UMI had a higher mortality than patients with no MI. It is not known whether secondary prevention would be useful in UMI patients. Cardiovascular magnetic resonance has made an enormous contribution to the diagnosis and management of the cardiomyopathies through the presence and patterns of myocardial fibrosis from LGE imaging, tissue characterization through T1, T2, and T2\* mapping, and accurate measures of ventricular function and mass. Gutman et al.<sup>15</sup> studied 452 patients with non-ischaemic dilated cardiomyopathy (DCM) stratified by the presence or absence of non-ischaemic myocardial fibrosis by LGE. In patients with fibrosis, the mortality was reduced by an implantable cardioverter-defibrillator (ICD) with HR 0.45 ( $P = 0.003$ ), but in patients without fibrosis there was no improvement in mortality with ICD (HR 1.22,  $P = 0.64$ ). The authors conclude that in non-ischaemic DCM, the presence of fibrosis may allow for improved selection of patients requiring ICD. Galan-Arriola et al.<sup>16</sup> used serial CMR to identify the early stages of anthracycline-induced cardiotoxicity in a pig study. The earliest detectable abnormality was increased T2 relaxation which was correlated on histology with intramyocyte oedema, with-

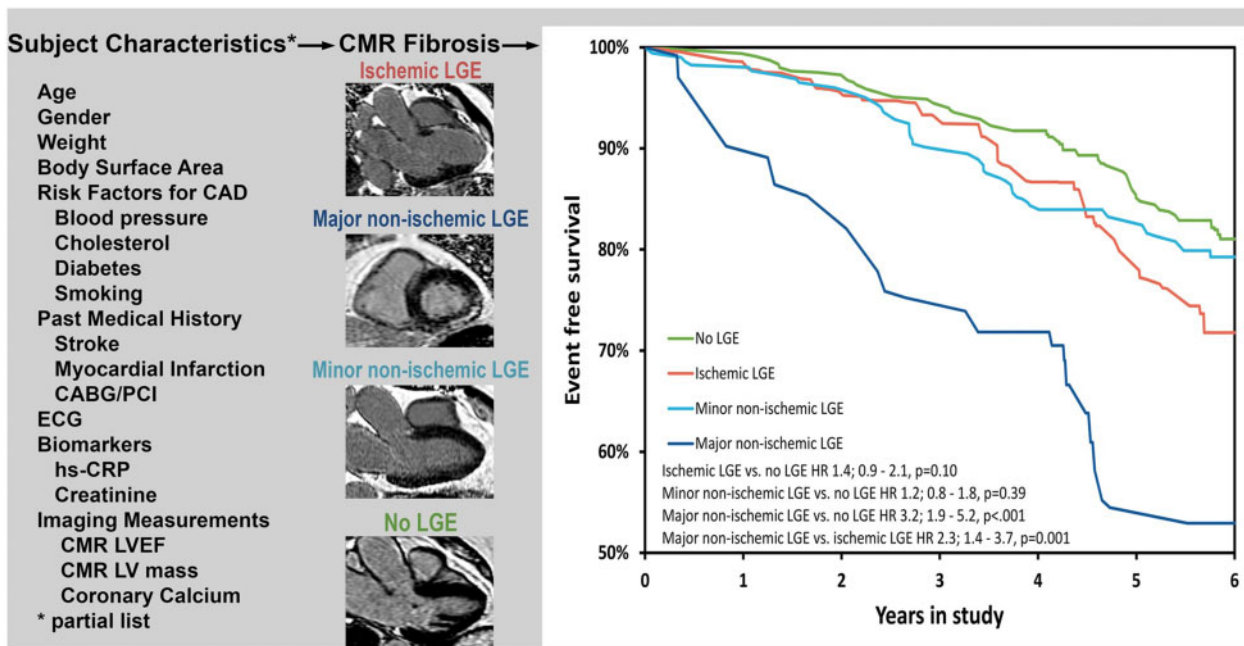


**Figure 2** Inverse propensity adjusted prognosis of ischaemic and non-ischaemic myocardial fibrosis. Reproduced with permission from Shanbhag et al.<sup>13</sup>

out change in the extracellular space. Changes in T1 and the extracellular volume on T1 mapping occurred much later and coincided with wall motion abnormalities. Stopping doxorubicin upon detection of T2 abnormality resolved intramyocyte vacuolization, indicating that the early T2 findings are at a stage when reversibility is still possible. These findings have important clinical implications for cancer therapy. Scally *et al.*<sup>17</sup> studied 55 patients with takotsubo cardiomyopathy using CMR including ultrasmall paramagnetic particles of iron oxide (USPIO) which localize in inflammatory macrophages. During the acute presentation, USPIO signal was reduced in the ballooning zone by 27% ( $P < 0.001$ ) as compared to non-ballooning zone (19%  $P = 0.02$ ). No enhancement was visible in either zone at 5 months. The authors conclude that takotsubo cardiomyopathy is characterized by an acute myocardial macrophage inflammatory infiltrate, most marked in the ballooning zone. Aung *et al.*<sup>18</sup> report on 3920 subjects from the UK Biobank study who were free of overt cardiovascular disease but had chronic exposure to ambient air pollutants including particulates and nitrogen dioxide. There was an incremental increase in LV and RV end-diastolic and LV endsystolic volumes with increasing exposure to particulates with a diameter of  $< 2.5 \mu\text{m}$ . Likewise, biventricular volumes were increased with higher nitrogen dioxide exposure. The authors conclude that air pollution is an under-recognized cardiac risk factor that may contribute to heart failure.

Diffusion tensor (DT) CMR is a new technique that images the asymmetry of water diffusion to define tissue architecture. Tissue such as neurons and the myocardium can be interrogated because of their longitudinal grain. The technique has recently become possible *in vivo* in humans and has been well validated. The three-dimensional (3D) architecture of the layers of the heart is now well described and is preserved across mammalian species suggesting

that the observed structure has functional importance. Khalique *et al.*<sup>19</sup> report the first series of patients in whom the 3D architecture is deranged, these being those with situs inversus totalis (SIT, dextrocardia). The normal epicardial left-handed myocyte helix was switched to right handed at the base with a return to left handed at the apex. The endocardium was likewise inverted at the base, with variable derangement more apically. There was reduced strain in the SIT hearts. The long-term consequences of these findings are not yet known, but it could be hypothesized that SIT patients may be more susceptible to heart failure from a second insult such as hypertension or infarction. Ariga *et al.*<sup>20</sup> used DT-CMR to examine 50 patients with hypertrophic cardiomyopathy and report a reduction in the diffusion parameter called fractional anisotropy (FA) in patients with ventricular arrhythmias [odds ratio (OR) 2.5,  $P = 0.015$ ]. Fractional anisotropy reflects packing of the myocytes and could therefore be reduced in myocardial disarray. Whilst there is no direct evidence of this from histology, the authors conclude that connection of reduced FA with arrhythmias might reflect disarray. Further work is needed to validate this intriguing study.

Cardiovascular magnetic resonance has been used for decades to image the aorta and the aortic valve. Musa *et al.*<sup>21</sup> report on 674 patients with severe aortic stenosis who also underwent LGE CMR at six UK centres. The presence and extent of myocardial fibrosis independently predicted mortality with a two-fold increase in late mortality. Guala *et al.*<sup>22</sup> report on 117 Marfan patients in a multicentre study of outcome. During 86 months of follow-up, the growth rate of the aortic diameter was 0.62 mm/year, and events were independently predicted by the proximal aorta longitudinal strain. The authors suggest that this simple measure could be included in risk assessment of Marfan patients.

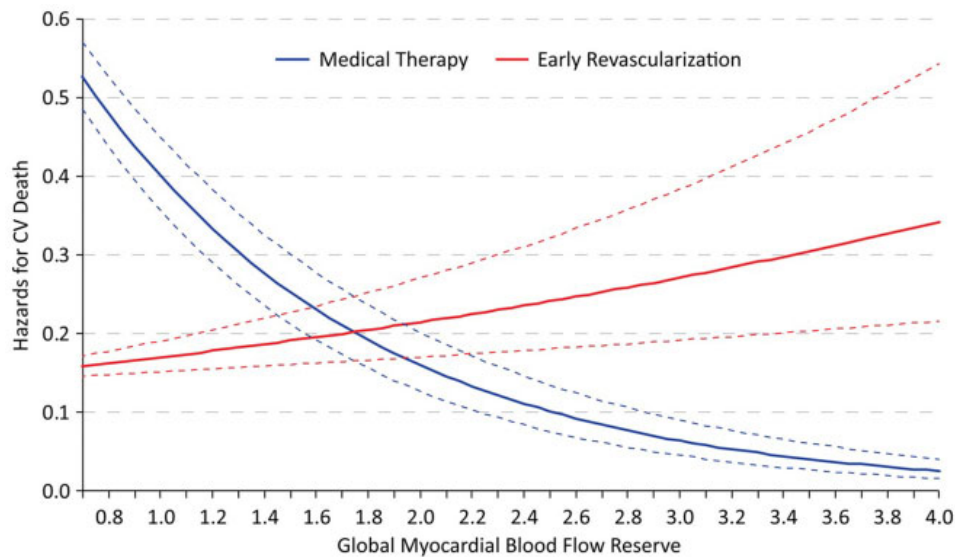


**Figure 3** Hazards for cardiac death with early revascularization compared to medical therapy based on global myocardial blood flow reserve by positron emission tomography myocardial perfusion imaging. Reproduced with permission from Patel et al.<sup>26</sup>

## Nuclear imaging

The current limitation of coronary computed tomography angiography (CCTA) is its suboptimal positive predictive value for the identification of myocardial ischaemia. Myocardial perfusion imaging (MPI) using CT could solve that limitation. Alessio *et al.*<sup>23</sup> performed a dynamic contrast-enhanced cardiac CT and <sup>82</sup>rubidium positron emission tomography (PET) imaging in 34 high-risk patients. The CT-derived global myocardial blood flow values correlated highly with those measured on PET ( $r = 0.92$ ;  $P < 0.001$ ). In addition, the mean global myocardial blood flow values estimated on CT vs. PET were comparable ( $0.9 \pm 0.3$  vs.  $1.0 \pm 0.2$  mL/min/g at rest and  $2.1 \pm 0.7$  vs.  $2.0 \pm 0.8$  mL/min/g during stress, respectively). However, myocardial blood flow estimates on CT contained substantial individual variance with a standard error of the estimate of 0.44 mL/min/g. The results are promising but further development is needed to improve reliability of the methodology at individual level as well. Furthermore, the study measured only global perfusion, while regional values would be more clinically meaningful. Another novel method to determine whether a coronary lesion is functionally significant is transmural attenuation gradient (TAG) that can be measured using standard CCTA data. In the presence of significant coronary stenosis, luminal attenuation will decrease rapidly on CCTA and can be measured with TAG. In the study by Bom *et al.*<sup>24</sup> Transmural attenuation gradient was compared against quantitative PET perfusion imaging and invasive fractional flow reserve (FFR) and demonstrated that TAG did not discriminate between vessels with or without ischaemia as defined by either PET or FFR. The lack of diagnostic value of TAG was related to the large variability of coronary luminal dimensions.

Artificial intelligence is currently a hot topic in medical image analysis. Machine learning, especially deep learning has been shown to be promising in disease detection and classification using image data. Betancur *et al.*<sup>25</sup> explored

deep learning for automatic prediction of obstructive CAD from the polar plots of single photon emission CT (SPECT) MPI in 1638 patients with suspected CAD. The area under the receiver operating characteristic curve for disease prediction by deep learning was higher than that of the standard analysis (per patient: 0.80 vs. 0.78; per vessel: 0.76 vs. 0.73;  $P < 0.01$ ). The results demonstrate that deep learning has the potential to perform automatic interpretation of MPI images with at least the same accuracy than the standard analysis.

While the diagnostic and prognostic power of MPI has been well characterized, there is little evidence on how this information should guide patient management. Patel *et al.*<sup>26</sup> examined a cohort of 12 594 patients with suspected or known CAD undergoing PET MPI. The patients were followed-up for 3.2 years. As expected, the low global perfusion reserve was associated with greater hazard of all-cause death. More interestingly, the patients with global perfusion reserve

$\leq 1.8$  had a survival benefit with early revascularization, regardless of the level of regional ischaemia. However, the patients with preserved perfusion reserve had no benefit of revascularization over medical therapy (Figure 3).<sup>26</sup> The results are concordant with earlier findings showing that large ischaemia justifies revascularization<sup>27,28</sup> and extend this notion also to global myocardial perfusion reserve.

<sup>18</sup>F-fluoride PET imaging is gaining increasing interest in various conditions as an indicator of tissue microcalcification, which is occurring in atherosclerosis. Creager *et al.*<sup>29</sup> investigated in an *ex vivo* study if <sup>18</sup>F-fluoride accumulation on atherosclerotic plaques are related to the development of microcalcifications that are not visible on CT. In this complex study, <sup>18</sup>F-fluoride signal in tissue analysis of human and mouse specimens was found to be clearly linked with small microcalcifications, which were not detected on CT. These results confirm that plaque mineralization is an active process and that <sup>18</sup>F-fluoride PET imaging detects coronary and carotid plaques with high-risk features.

In the study by Carlidge *et al.*,<sup>30</sup> the degeneration of bio-

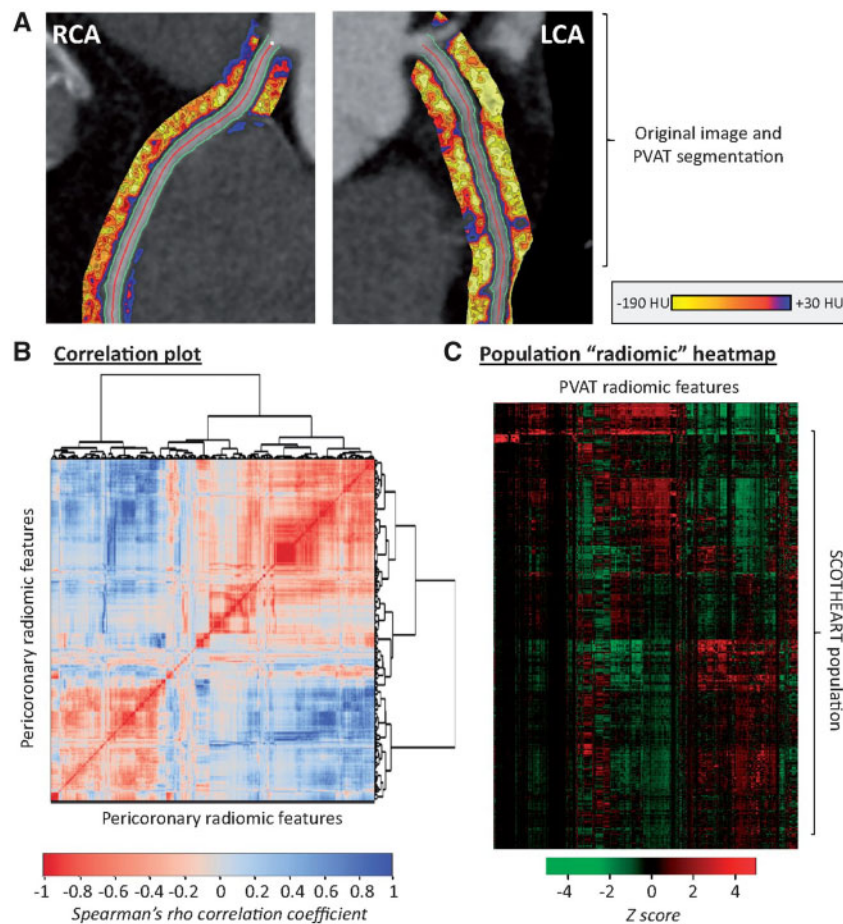


**Figure 4** Radiomic phenotyping of coronary perivascular adipose tissue. (A) The perivascular adipose tissue (PVAT) of the right (RCA) and left (LCA) coronary was segmented and used to calculate a number of shape-, attenuation-, and texture-related statistics. (B) Correlation plot of all 1391 stable radiomic features in the SCOT-HEART population ( $n=1575$  patients), with hierarchical clustering revealing distinct clusters of radiomic variance. (C) Heatmap of scaled radiomic features in the SCOT-HEART population revealing between-patient variance across the cohort. Reproduced with permission from Oikonomou *et al.*<sup>44</sup>

prosthetic aortic valve was investigated using  $^{18}\text{F}$ -fluoride PET. In *ex vivo* analyses, the  $^{18}\text{F}$ -fluoride uptake colocalized with tissue degeneration on histology. In patients with aortic bioprostheses, increased valve  $^{18}\text{F}$ -fluoride uptake in PET imaging was associated with more rapid deterioration in valve function at 2-year follow-up. Aortic bioprosthesis dysfunction was detected in 10 patients and all of them showed  $^{18}\text{F}$ -fluoride uptake at baseline when still the valve haemodynamics were normal. On multivariable analysis,  $^{18}\text{F}$ -fluoride uptake was the only independent predictor of future bioprosthetic dysfunction. Although a larger patient cohort is needed,  $^{18}\text{F}$ -fluoride PET imaging appears promising method in predicting dysfunction of bioprosthetic valves.

Infection and inflammation imaging using molecular imaging methods is an established technique in prosthetic valve endocarditis and device infections. Swart *et al.*<sup>31</sup> investigated the possible confounders that may impact on the accuracy of  $^{18}\text{F}$ -fluoro-deoxyglucose (FDG) PET/CT. In a multicentre study, 160 patients with suspected prosthetic valve endocarditis and 77 control patients were scanned. The authors found that low inflammatory activity (C-reactive protein  $<40$  mg/L)—possibly linked with prolonged antibiotic therapy at the time of imaging—and use of surgical adhesives during prosthetic heart valve

implantation were significant confounders, whereas recent valve implantation was not.

Another challenging population is patients with suspected infection of cardiac implantable electronic devices. In a study by Calais *et al.*,<sup>32</sup> the diagnostic positive and negative predictive values were 80% and 91% for FDG PET and 100% and 85% for white blood cell SPECT, respectively. A prolonged antibiotic therapy before imaging tended to decrease the sensitivity for both techniques. As FDG is not specific for inflammation but for glucose uptake, more specific imaging agents for infection are being developed.

## Computed tomography

Cardiac computed tomography has evolved into a one-stop-shop imaging tool that can provide valuable diagnostic and prognostic information in patients with suspected or known CAD. Assessment of coronary artery calcium (CAC) score on CT can be used as a risk modifier and may guide statin therapy. Mitchel *et al.*<sup>33</sup> assessed the relative impact of statins on adverse cardiovascular events stratified by CAC scores in 13 644 patients (mean age 50 years; 71% men) who were followed-up for a median of 9.4 years. Patients without CAC had an excellent prognosis irrespective of statin therapy whereas in patients

with CAC > 0 statin therapy was associated with reduced risk of major adverse cardiovascular events (adjusted subHR 0.76; 95% CI 0.60–0.95;  $P = 0.015$ ). The effect of statin use on major adverse cardiovascular events was significantly related to the severity of CAC ( $P < 0.0001$  for interaction), with a number needed to treat to prevent 1 initial major adverse cardiovascular events over 10 years ranging from 100 (when CAC was 1–100) to 12 (if CAC > 100). A recent *post hoc* analysis of the SCOT-HEART trial demonstrated that coronary heart disease death or non-fatal MI was three times more frequent in patients with high-risk plaque features (positive remodelling or low attenuation plaque) and was twice as frequent in those with obstructive CAD.<sup>34</sup> However, these associations were not independent of CAC score, a surrogate measure of atherosclerosis burden.

The investigators of the PROMISE Trial assessed the prevalence and clinical predictors of high-risk CAD (defined as left main stenosis or either  $\geq 50\%$  stenosis or  $\geq 70\%$  stenosis of 3 vessels or 2-vessel CAD involving the proximal left anterior descending artery).<sup>35</sup> High-risk CAD was identified in 6.6% ( $\geq 50\%$  stenosis) and 2.4% ( $\geq 70\%$  stenosis) of patients. Variables predictive of high-risk CAD included family history of premature CAD, age, male sex, lower glomerular filtration rate, diabetes mellitus, elevated systolic blood pressure, and angina. High-risk CAD was associated with more frequent invasive interventions and adverse events as compared to non-high-risk CAD.

An intriguing study has investigated the prognostic value of combined information of lesion-specific ischaemia (FFR) and adverse plaque features by CCTA.<sup>36</sup> The authors evaluated 772 vessels (299 patients) by both CCTA and invasive FFR measurement. Interestingly, the presence of  $\geq 3$  high-risk plaque features was independently associated with clinical events in the FFR > 0.80 group, but not in the FFR  $\leq 0.80$  group. It seems that the integration of both lesion-specific ischaemia and CT plaque features may provide better prognostic stratification than either individual component alone, especially in patients with  $n$  FFR > 0.80. Using computational fluid dynamics simulations CT is now capable to provide non-invasive FFR measurements. A study by Norgaard *et al.*<sup>37</sup> assessed real-world clinical outcomes following a diagnostic strategy including first-line coronary CTA with selective FFR<sub>CT</sub> testing. The study reviewed the results of 3674 consecutive patients with stable chest pain evaluated with CTA and FFR<sub>CT</sub> testing. The presence of intermediate-range CAD and FFR<sub>CT</sub> > 0.80 was associated with favourable clinical outcomes similar to the prognosis in patients without or with minimal evidence of CAD. Beyond FFR<sub>CT</sub> simulation stress CT perfusion has emerged as a potential strategy to acquire anatomic and functional evaluation of CAD. Whole heart coverage CT scanners have become readily available, which allow a more robust stress CT MPI (CTP). The diagnostic accuracy of latest scanner generation was tested by Pontone *et al.*<sup>38</sup> in 100 intermediate to high-risk symptomatic patients with suspected CAD. CCTA alone demonstrated a sensitivity, specificity, negative predictive value, positive predictive value, and accuracy of 98%, 76%, 99%, 63%, and 83%, respectively. Combining CCTA with stress CTP, these values were 91%, 94%, 96%, 86%, and 93%, respectively, with a

significant improvement in specificity, positive predictive value, and accuracy. The mean effective radiation dose for CCTA and stress CTP were  $2.8 \pm 1.4$  mSv and  $2.5 \pm 1.1$  mSv. Patients with diabetes are a high-risk patient cohort for adverse cardiovascular outcomes. The PROMISE Trial investigators assessed whether a diagnostic strategy based on CCTA is superior to functional stress testing in reducing cardiovascular death or MI among symptomatic patients with diabetes [ $n = 1908$  (21%)] vs. patients without diabetes [ $n = 7058$  (79%)].<sup>39</sup> Patients with diabetes who underwent CCTA had a lower risk of cardiovascular death or MI compared with functional stress testing [CCTA: 1.1% (10 of 936) vs. stress testing: 2.6% (25 of 972); adjusted HR 0.38; 95% CI 0.18–0.79;  $P = 0.01$ ]. Another study including also individuals with diabetes, investigated the rate and extent of plaque progression, changes in plaque features, and clinical predictors of plaque progression.<sup>40</sup> A total of 1602 patients who underwent serial CCTA (median scan interval 3.8 years) were enrolled and analysed from the PARADIGM (Progression of Atherosclerotic Plaque Determined by Computed Tomographic Angiography Imaging) trial.<sup>41</sup> Diabetes was an independent risk factor for plaque progression (OR 1.526, 95% CI 1.100–2.118;  $P = 0.011$ ).

A more precise risk assessment that incorporates the detection of coronary inflammation would allow personalized medical interventions. Novel analytical techniques such as perivascular fat attenuation index or plaque-based radiomics may facilitate the detection and quantification of pericoronary inflammation and atherosclerotic plaque activity.<sup>42,43</sup> An innovative study by Oikonomou *et al.*<sup>44</sup> demonstrated that artificial intelligence powered pericoronary fat radiomic profile (FRP) analysis significantly improved major adverse cardiovascular events prediction beyond traditional risk stratification that included risk factors, CAC, coronary stenosis, and high-risk plaque features on CCTA in the SCOT-HEART trial (Figure 4). The authors conclude that FRP leads to a significant improvement of cardiac risk prediction over and above the current state-of-the-art, which might help to identify patients with elevated residual risk for cardiovascular events.

## Advanced imaging, fusion imaging, and applied artificial intelligence in imaging

Cardiovascular (invasive and non-invasive) imaging is developing at a ultrafast pace and the clinician of today gets daily confronted with different imaging modalities, with major technological developments, but also fusion imaging and introduction of artificial intelligence and machine learning. From a clinical perspective, the cardiovascular imager of tomorrow needs to be familiar with the different modalities, when to apply which technique in which clinical scenario. A dedicated task force of The European Association of Cardiovascular Imaging (part of the ESC) has published a statement on the organization of multimodality imaging services in cardiology, the use of the different modalities as well as training and research in the multimodality era.<sup>1</sup>

Ramos *et al.*<sup>45</sup> used an animal (mice) model to study myocardial healing after infarction using serial imaging (7

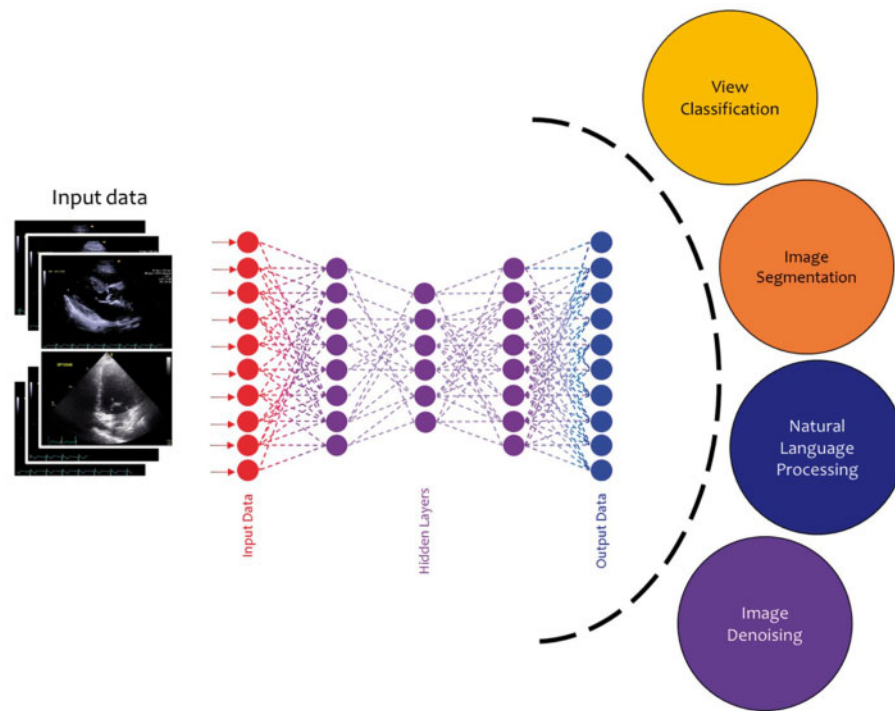


**Figure 5** Machine learning algorithms applied to echocardiography. Echocardiographic data are post-processed to automate many processes performed in clinical practice by cardiologists and sonographers such as view classification and image segmentation that will lead to the interpretation of the data and the diagnosis. Reproduced with permission from Al'Aref *et al.*<sup>49</sup>

days and 21 days postinfarction) with 3 T magnetic resonance imaging (MRI) and a 19F/1H surface coil. Injected 19F-perfluorocarbon nanoparticles were used to evaluate recruitment of inflammatory cells (e.g. macrophages), and an injected gadolinium-based elastin-binding contrast agent was used to assess elastin content. The combination of these imaging techniques enabled assessing the time course of the remodelling and healing process, as well as scar development.

Engel *et al.*<sup>46</sup> evaluated 25 patients with either stable CAD or presenting with suspected ACS using a non-invasive albumin-binding probe gadofosveset-enhanced CMR, as well as invasive coronary angiography and optical coherence tomography (OCT). CMR was performed twice: prior to baseline examination and 24 h after gadofosveset-trisodium administration. The patients with suspected ACS revealed significantly higher signal enhancement on CMR following gadofosveset-trisodium application on the segments containing culprit lesion as compared to patients with stable CAD. On OCT, these patients presented with thin-cap fibroatheroma. The novel CMR approach may enable early detection of patients with potential ACS.

Several articles in the field of multimodality and fusion imaging are worth to highlight. Mitral annular calcification is observed in patients with mitral regurgitation/stenosis and is important when transcatheter valve replacement is considered. To better understand pathophysiology, Massera *et al.*<sup>47</sup> performed CT calcium score of the mitral annulus, as well as PET with <sup>18</sup>F-fluoride (calcification activity) and <sup>18</sup>F-FDG (inflammation activity) in 104 patients. Mitral annular calcification was noted in 35 patients who exhibited increased <sup>18</sup>F-fluoride uptake and FDG uptake, suggesting increased local calcification and inflammation.

Fernandez-Friera *et al.*<sup>48</sup> used hybrid FDG PET/MRI to assess arterial vascular plaques in middle-aged individuals ( $n = 755$ ). With this sophisticated imaging technology, the authors evaluated multiterritorial atherosclerosis (carotid, aortic, and ilio-femoral arteries); plaques were present on MRI in 90.1% (73.9% femorals, 55.8% iliacs, and 53.1% carotids), whereas inflammation was observed on PET in 48.2% of individuals (24.4% femorals, 19.3% aorta, 15.8% carotids, and 9.3% iliacs). The authors concluded that arterial inflammation is noted in 50% of arterial plaques in middle-aged individuals.

The current status of artificial intelligence and machine learning was elegantly reviewed by Al'Aref *et al.*<sup>49</sup> With the increasing digitization of data making big datasets available and easier to process, machine learning has enabled to autonomously acquire knowledge by the extraction of patterns from these large datasets. Particularly in cardiology machine learning has been rapidly adopted in various fields, to permit automated analysis of electrocardiograms and imaging (echocardiography, nuclear perfusion imaging, and CCTA) (Figure 5).

Another excellent review was published by Krittanawong *et al.*<sup>2</sup> providing further insight in deep learning. This is a branch of artificial intelligence, which combines computer science, statistics and decision theory to discover patterns in complex and big data. Casaclang-Verzosa *et al.*<sup>50</sup> applied machine learning to advanced network analysis to demonstrate automated assessment of LV (hypertrophy) in response to aortic valve stenosis from echocardiographic images. Finally, Zhang *et al.*<sup>51</sup> published original research on the use of deep learning to analyse echocardiographic data ( $n = 14\ 035$  echocardiograms), in a fully automated fashion, including (i) view identifica-

tion, (ii) image segmentation, (iii) quantification of structure and function, and (iv) disease detection. Specifically, convolutional neural networks were trained to detect hypertrophic cardiomyopathy, cardiac amyloidosis, and pulmonary arterial hypertension with respective C statistics of 0.93, 0.87, and 0.85.

Conflict of interest: The Department of Cardiology of the Leiden University Medical Center received unrestricted research grants from Biotronik, Bioventrix, Boston Scientific, Edwards Lifesciences, Medtronic and GE Healthcare. J.J.B. received speaker fees from Abbott Vascular. V.D. received speaker fees from Abbott Vascular and Medtronic. D.P. reports research support from Siemens, grants from La Jolla, grants from Bayer, grants and personal fees from ApoPharma. The remaining authors have nothing to disclose.

## References

- Fox K, Achenbach S, Bax J, Cosyns B, Delgado V, Dweck MR, Edvardsen T, Flachskampf F, Habib G, Lancellotti P, Muraru D, Neglia D, Pontone G, Schwammenthal E, Sechtem U, Westwood M, Popescu BA. Multimodality imaging in cardiology: a statement on behalf of the Task Force on Multimodality Imaging of the European Association of Cardiovascular Imaging. *Eur Heart J* 2019;40:553–558.
- Krittana Wong C, Johnson KW, Rosenson RS, Wang Z, Aydar M, Baber U, Min JK, Tang WHW, Halperin JL, Narayan SM. Deep learning for cardiovascular medicine: a practical primer. *Eur Heart J* 2019;40:2058–2073.
- Lassen MCH, Biering-Sørensen SR, Olsen FJ, Skaarup KG, Tolstrup K, Qasim AN, Møgelvang R, Jensen JS, Biering-Sørensen T. Ratio of transmitral early filling velocity to early diastolic strain rate predicts long-term risk of cardiovascular morbidity and mortality in the general population. *Eur Heart J* 2019;40:518–525.
- Modin D, Biering-Sørensen SR, Møgelvang R, Jensen JS, Biering-Sørensen T. Prognostic importance of left ventricular mechanical dyssynchrony in predicting cardiovascular death in the general population. *Circ Cardiovasc Imaging* 2018;11: e007528.
- Wehner GJ, Jing L, Haggerty CM, Suever JD, Leader JB, Hartzel DN, Kirchner HL, Manus JNA, James N, Ayar Z, Gladding P, Good CW, Cleland JGF, Fornwalt BK. Routinely reported ejection fraction and mortality in clinical practice: where does the nadir of risk lie? *Eur Heart J* 2019;doi: 10.1093/eurheartj/ehz550.
- Ghimire A, Fine N, Ezekowitz JA, Howlett J, Youngson E, McAlister FA. Frequency, predictors, and prognosis of ejection fraction improvement in heart failure: an echocardiogram-based registry study. *Eur Heart J* 2019;40:2110–2117.
- Obokata M, Reddy YNV, Melenovsky V, Pislaru S, Borlaug BA. Deterioration in right ventricular structure and function over time in patients with heart failure and preserved ejection fraction. *Eur Heart J* 2019;40:689–697.
- Freed BH, Daruwalla V, Cheng JY, Aguilar FG, Beussink L, Choi A, Klein DA, Dixon D, Baldrige A, Rasmussen-Torvik LJ, Maganti K, Shah SJ. Prognostic utility and clinical significance of cardiac mechanics in heart failure with preserved ejection fraction: importance of left atrial strain. *Circ Cardiovasc Imaging* 2016;9.
- Vollema EM, Sugimoto T, Shen M, Tastet L, Ng ACT, Abou R, Marsan NA, Mertens B, Dulgheru R, Lancellotti P, Clavel MA, Pibarot P, Genereux P, Leon MB, Delgado V, Bax JJ. Association of left ventricular global longitudinal strain with asymptomatic severe aortic stenosis: natural course and prognostic value. *JAMA Cardiol* 2018;3:839–847.
- Bartko PE, Arfsten H, Heitzinger G, Pavo N, Toma A, Strunk G, Hengstenberg C, Hulsmann M, Goliash G. A unifying concept for the quantitative assessment of secondary mitral regurgitation. *J Am Coll Cardiol* 2019;73:2506–2517.
- Nazerian P, Mueller C, Vanni S, Soeiro AM, Leidel BA, Cerini G, Lupia E, Palazzo A, Grifoni S, Morello F. Integration of transthoracic focused cardiac ultrasound into the diagnostic algorithm for suspected acute aortic syndromes. *Eur Heart J* 2019;40:1952–1960.
- Chiesa ST, Masi S, Shipley MJ, Ellins EA, Fraser AG, Hughes AD, Patel RS, Khir AW, Halcox JP, Singh-Manoux A, Kivimaki M, Celermajer DS, Deanfield JE. Carotid artery wave intensity in mid to late-life predicts cognitive decline: the Whitehall II study. *Eur Heart J* 2019;40:2300–2309.
- Shanbhag SM, Greve AM, Aspelund T, Schelbert EB, Cao JJ, Danielsen R, Þorgeirsson G, Sigurðsson S, Eiríksdóttir G, Harris TB, Launer LJ, Guðnason V, Arai AE. Prevalence and prognosis of ischaemic and non-ischaemic myocardial fibrosis in older adults. *Eur Heart J* 2019;40:529–538.
- Acharya T, Aspelund T, Jonasson TF, Schelbert EB, Cao JJ, Sathya B, Dyke CK, Aletras AH, Sigurdsson S, Þorgeirsson G, Eiríksdóttir G, Harris T, Launer LJ, Guðnason V, Arai AE. Association of unrecognized myocardial infarction with long-term outcomes in community-dwelling older adults: the ICELAND MISTudy. *JAMA Cardiol* 2018;3:1101–1106.
- Gutman SJ, Costello BT, Papapostolou S, Voskoboinik A, Iles L, Ja J, Hare JL, Ellims A, Kistler PM, Marwick TH, Taylor AJ. Reduction in mortality from implantable cardioverter-defibrillators in non-ischaemic cardiomyopathy patients dependent on the presence of left ventricular scar. *Eur Heart J* 2019;40: 542–550.
- Galan-Arriola C, Lobo M, Vilchez-Tschischke JP, Lopez GJ, de Molina-Iracheta A, Perez-Martinez C, Agüero J, Fernandez-Jimenez R, Martín-García A, Oliver E, Villena-Gutiérrez R, Pizarro G, Sanchez PL, Fuster V, Sanchez-Gonzalez J, Ibanez B. Serial magnetic resonance imaging to identify early stages of anthracycline-induced cardiotoxicity. *J Am Coll Cardiol* 2019;73:779–791.
- Scally C, Abbas H, Ahearn T, Srinivasan J, Mezincescu A, Rudd A, Spath N, Yucel-Finn A, Yucel R, Oldroyd K, Dospinescu C, Horgan G, Broadhurst P, Henning A, Newby DE, Semple S, Wilson HM, Dawson DK. Myocardial and systemic inflammation in acute stress-induced (takotsubo) cardiomyopathy. *Circulation* 2019;139:1581–1592.
- Aung N, Sanghvi MM, Zemrak F, Lee AM, Cooper JA, Paiva JM, Thomson RJ, Fung K, Khanji MY, Lukaschuk E, Carapella V, Kim YJ, Munroe PB, Piechnik SK, Neubauer S, Petersen SE. Association between ambient air pollution and cardiac morpho-functional phenotypes: insights from the UK biobank population imaging study. *Circulation* 2018;138:2175–2186.
- Khalique Z, Ferreira PF, Scott AD, Nielles-Vallespin S, Kilner PJ, Kutys R, Romero M, Arai AE, Firmin DN, Pennell DJ. Deranged myocyte microstructure in situs inversus totalis demonstrated by diffusion tensor cardiac magnetic resonance. *JACC Cardiovasc Imaging* 2018;11:1360–1362.
- Ariga R, Tunnicliffe EM, Manohar SG, Mahmod M, Raman B, Piechnik SK, Francis JM, Robson MD, Neubauer S, Watkins H. Identification of myocardial disarray in patients with hypertrophic cardiomyopathy and ventricular arrhythmias. *J Am Coll Cardiol* 2019;73:2493–2502.
- Musa TA, Treibel TA, Vassiliou VS, Captur G, Singh A, Chin C, Dobson LE, Pica S, Loudon M, Malley T, Rigolli M, Foley JRJ, Bijsterveld P, Law GR, Dweck MR, Myerson SG, McCann GP, Prasad SK, Moon JC, Greenwood JP. Myocardial scar and mortality in severe aortic stenosis. *Circulation* 2018;138:1935–1947.
- Guala A, Teixidó-Tura G, Rodríguez-Palomares J, Ruiz-Muñoz A, Dux-Santoy L, Villalva N, Granato C, Galian L, Gutiérrez L, González-Alujas T, Sanchez V, Forteza A, García-Dorado D, Evangelista A. Proximal aorta longitudinal strain predicts aortic root dilation rate and aortic events in Marfan syndrome. *Eur Heart J* 2019;40:2047–2055.
- Alessio AM, Bindschadler M, Busey JM, Shuman WP, Caldwell JH, Branch KR. Accuracy of myocardial blood flow estimation from dynamic contrast-enhanced cardiac CT compared with PET. *Circ Cardiovasc Imaging* 2019;12:e008323.
- Bom MJ, Driessen RS, Stuijzand WJ, Raijmakers PG, Van Kuijk CC, Lammermsma AA, van Rossum AC, van Royen N, Knuuti J, Maki M, Nieman K, Min JK, Leipsic JA, Danad I, Knaapen P. Diagnostic value of transluminal attenuation gradient for the presence of ischemia as defined by fractional flow reserve and quantitative positron emission tomography. *JACC Cardiovasc Imaging* 2019;12:323–333.
- Betancur J, Commandeur F, Motlagh M, Sharir T, Einstein AJ, Bokhari S, Fish MB, Ruddy TD, Kaufmann P, Sinusas AJ, Miller EJ, Bateman TM, Dorbala S, Di Carli M, Germano G, Otaki Y, Tamarappoo BK, Dey D, Berman DS, Slomka PJ. Deep learning for prediction of obstructive disease from fast myocardial perfusion SPECT: a multicenter study. *JACC Cardiovasc Imaging* 2018;11:1654–1663.
- Patel KK, Spertus JA, Chan PS, Sperry BW, Al Badarin F, Kennedy KF, Thompson RC, Case JA, McGhie AI, Bateman TM. Myocardial blood flow reserve assessed by positron emission tomography myocardial perfusion imaging identifies patients with a survival benefit from early revascularization. *Eur Heart J* 2019;doi: 10.1093/eurheartj/ehz389.
- Hachamovitch R, Rozanski A, Shaw LJ, Stone GW, Thomson LE, Friedman JD, Hayes SW, Cohen I, Germano G, Berman DS. Impact of ischaemia and scar on the therapeutic benefit derived from myocardial revascularization vs. medical therapy among patients undergoing stress-rest myocardial perfusion scintigraphy. *Eur Heart J* 2011;32:1012–1024.

28. Neglia D, Liga R, Caselli C, Carpeggiani C, Lorenzoni V, Sicari R, Lombardi M, Gaemperli O, Kaufmann PA, Scholte A, Underwood SR, Knuuti J; EVINCI Study Investigators. Anatomical and functional coronary imaging to predict long-term outcome in patients with suspected coronary artery disease: the EVINCIOutcome study. *Eur Heart J Cardiovasc Imaging* 2019;doi: 10.1093/ehjci/jez248.
29. Creager MD, Hohl T, Hutcheson JD, Moss AJ, Schlotter F, Blaser MC, Park MA, Lee LH, Singh SA, Alcaide-Corral CJ, Tavares AAS, Newby DE, Kijewski MF, Aikawa M, Di Carli M, Dweck MR, Aikawa E. (18)F-fluoride signal amplification identifies microcalcifications associated with atherosclerotic plaque instability in positron emission tomography/computed tomography images. *Circ Cardiovasc Imaging* 2019;12:e007835.
30. Cartledge TRG, Doris MK, Sellers SL, Pawade TA, White AC, Pessotto R, Kwicinski J, Fletcher A, Alcaide C, Lucatelli C, Densem C, Rudd JHF, van Beek EJ, Tavares A, Virmani R, Berman D, Leipsic JA, Newby DE, Dweck MR. Detection and prediction of bioprosthetic aortic valve degeneration. *J Am Coll Cardiol* 2019;73:1107–1119.
31. Swart LE, Gomes A, Scholtens AM, Sinha B, Tanis W, Lam M, van der Vlugt MJ, Streukens SAF, Aarntzen E, Bucerius J, van Assen S, Bleeker-Rovers CP, van Geel PP, Krestin GP, van Melle JP, Roos-Hesselink JW, Slart R, Glaudemans A, Budde R. Improving the diagnostic performance of (18)F-fluorodeoxyglucose positron-emission tomography/computed tomography in prosthetic heart valve endocarditis. *Circulation* 2018;138:1412–1427.
32. Calais J, Touati A, Grall N, Laouenan C, Benali K, Mahida B, Vigne J, Hyafil F, LungB, Duval X, Lepage L, Le Guludec D, Rouzet F. Diagnostic impact of (18)F-fluorodeoxyglucose positron emission tomography/computed tomography and white blood cell SPECT/computed tomography in patients with suspected cardiac implantable electronic device chronic infection. *Circ Cardiovasc Imaging* 2019;12:e007188.
33. Mitchell JD, Fergestrom N, Gage BF, Paisley R, Moon P, Novak E, Cheezum M, Shaw LJ, Villines TC. Impact of statins on cardiovascular outcomes following coronary artery calcium scoring. *J Am Coll Cardiol* 2018;72:3233–3242.
34. Williams MC, Moss AJ, Dweck M, Adamson PD, Alam S, Hunter A, Shah ASV, Pawade T, Weir-McCall JR, Roditi G, van Beek EJ, Newby DE, Nicol ED. Coronary artery plaque characteristics associated with adverse outcomes in theSCOT-HEART study. *J Am Coll Cardiol* 2019;73:291–301.
35. Jang JJ, Bhapkar M, Coles A, Vemulapalli S, Fordyce CB, Lee KL, Udelsion JE, Hoffmann U, Tardif JC, Jones WS, Mark DB, Sorrell VL, Espinoza A, Douglas PS, Patel MR; PROMISE Investigators. Predictive model for high-risk coronary artery disease. *Circ Cardiovasc Imaging* 2019;12:e007940.
36. Lee JM, Choi KH, Koo BK, Park J, Kim J, Hwang D, Rhee TM, Kim HY, Jung HW, Kim KJ, Yoshiaki K, Shin ES, Doh JH, Chang HJ, Cho YK, Yoon HJ, Nam CW, Hur SH, Wang J, Chen S, Kuramitsu S, Tanaka N, Matsuo H, Akasaka T. Prognostic implications of plaque characteristics and stenosis severity in patients with coronary artery disease. *J Am Coll Cardiol* 2019;73:2413–2424.
37. Norgaard BL, Terkelsen CJ, Mathiassen ON, Grove EL, Botker HE, Parner E, Leipsic J, Steffensen FH, Riis AH, Pedersen K, Christiansen EH, Maeng M, Krusel LR, Kristensen SD, Eftekhari A, Jakobsen L, Jensen JM. Coronary CT angiographic and flow reserve-guided management of patients with stable ischemic heart disease. *J Am Coll Cardiol* 2018;72:2123–2134.
38. Pontone G, Andreini D, Guaricci A, Baggiano A, Fazzari F, Guglielmo M, Muscogiuri G, Berzovini CM, Pasquini A, Mushtaq S, Conte E, Calligaris G, De Martini S, Ferrari C, Galli S, Grancini L, Ravagnani P, Teruzzi G, Trabattoni D, Fabbicocchi F, Lualdi A, Montorsi P, Rabbat MG, Bartorelli AL, Pepi M. Incremental diagnostic value of stress computed tomography myocardial perfusion with whole-heart coverage CT scanner in intermediate to high-risk symptomatic patients suspected of coronary artery disease. *JACC Cardiovasc Imaging* 2019;12:338–349.
39. Sharma A, Coles A, Sekaran NK, Pagidipati NJ, Lu MT, Mark DB, Lee KL, Alkhalidi HR, Hoffmann U, Douglas PS. Stress testing versus CT angiography in patients with diabetes and suspected coronary artery disease. *J Am Coll Cardiol* 2019;73:893–902.
40. Lee SE, Sung JM, Andreini D, Budoff MJ, Cademartiri F, Chinnaiyan K, Choi JH, Chun EJ, Conte E, Gottlieb I, Hadamitzky M, Kim YJ, Kumar A, Lee BK, Leipsic JA, Maffei E, Marques H, Pontone G, Raff G, Shin S, Stone PH, Samady H, Virmani R, Narula J, Berman DS, Shaw LJ, Bax JJ, Lin FY, Min JK, Chang HJ. Differential association between the progression of coronary artery calcium score and coronary plaque volume progression according to statins: the Progression of Atherosclerotic Plaque Determined by Computed Tomographic Angiography Imaging (PARADIGM) study. *Eur Heart J Cardiovasc Imaging* 2019;20:1307–1314.
41. Lee SE, Chang HJ, Rizvi A, Hadamitzky M, Kim YJ, Conte E, Andreini D, Pontone G, Volpato V, Budoff MJ, Gottlieb I, Lee BK, Chun EJ, Cademartiri F, Maffei E, Marques H, Leipsic JA, Shin S, Choi JH, Chung N, Min JK. Rationale and design of the Progression of Atherosclerotic Plaque Determined by Computed Tomographic Angiography Imaging (PARADIGM) registry: a comprehensive exploration of plaque progression and its impact on clinical outcomes from a multicenter serial coronary computed tomographic angiography study. *Am Heart J* 2016;182:72–79.
42. Antoniadou C, Antonopoulos AS, Deanfield J. Imaging residual inflammatory cardiovascular risk. *Eur Heart J* 2019;doi: 10.1093/eurheartj/ehz474.
43. Kolossvary M, Park J, Bang JJ, Zhang J, Lee JM, Paeng JC, Merkely B, Narula J, Kubo T, Akasaka T, Koo BK, Maurovich-Horvat P. Identification of invasive and radionuclide imaging markers of coronary plaque vulnerability using radiomic analysis of coronary computed tomography angiography. *Eur Heart J Cardiovasc Imaging* 2019;20:1250–1258.
44. Oikonomou EK, Williams MC, Kotanidis CP, Desai MY, Marwan M, Antonopoulos AS, Thomas KE, Thomas S, Akoumianakis I, Fan LM, Kesavan S, Herdman L, Alashi A, Centeno EH, Lyasheva M, Griffin BP, Flamm SD, Shirodaria C, Sabharwal N, Kelion A, Dweck MR, Van Beek EJ, Deanfield J, Hopewell JC, Neubauer S, Channon KM, Achenbach S, Newby DE, Antoniadou C. A novel machine learning-derived radiotranscriptomic signature of perivascular fat improves cardiac risk prediction using coronary CT angiography. *Eur Heart J* 2019;doi: 10.1093/eurheartj/ehz592.
45. Ramos IT, Henningson M, Nezafat M, Lavin B, Llorio S, Gebhardt P, Protti A, Eykyn TR, Andia ME, Fogel U, Phinikaridou A, Shah AM, Botnar RM. Simultaneous assessment of cardiac inflammation and extracellular matrix remodeling after myocardial infarction. *Circ Cardiovasc Imaging* 2018;11.
46. Engel LC, Landmesser U, Gigengack K, Wurster T, Manes C, Girke G, Jaguszewski M, Skurk C, Leistner DM, Lauten A, Schuster A, Hamm B, Botnar RM, Makowski MR, Bigalke B. Novel approach for in vivo detection of vulnerable coronary plaques using molecular 3-T CMR imaging with an albumin-binding probe. *JACC Cardiovasc Imaging* 2019;12:297–306.
47. Massera D, Trivieri MG, Andrews JPM, Sartori S, Abgral R, Chapman AR, Jenkins WSA, Vesey AT, Doris MK, Pawade TA, Zheng KH, Kizer JR, Newby DE, Dweck MR. Disease activity in mitral annular calcification. *Circ Cardiovasc Imaging* 2019; 12:e008513.
48. Fernandez-Friera L, Fuster V, Lopez-Melgar B, Oliva B, Sanchez-Gonzalez J, Macias A, Perez-Asenjo B, Zamudio D, Alonso-Farto JC, Espana S, Mendiguren J, Bueno H, Garcia-Ruiz JM, Ibanez B, Fernandez-Ortiz A, Sanz J. Vascular inflammation in subclinical atherosclerosis detected by hybrid PET/MRI. *J Am Coll Cardiol* 2019;73:1371–1382.
49. Al'Aref SJ, Anchouche K, Singh G, Slomka PJ, Kolli KK, Kumar A, Pandey M, Maliakal G, van Rosendaal AR, Beecy AN, Berman DS, Leipsic J, Nieman K, Andreini D, Pontone G, Schoepf UJ, Shaw LJ, Chang HJ, Narula J, Bax JJ, Guan Y, Min JK. Clinical applications of machine learning in cardiovascular disease and its relevance to cardiac imaging. *Eur Heart J* 2019;40:1975–1986.
50. Casaclang-Verzosa G, Shrestha S, Khalil MJ, Cho JS, Tokodi M, Balla S, Alkhouli M, Badhwar V, Narula J, Miller JD, Sengupta PP. Network tomography for understanding phenotypic presentations in aortic stenosis. *JACC Cardiovasc Imaging* 2019;12:236–248.
51. Zhang J, Gajjala S, Agrawal P, Tison GH, Hallock LA, Beussink-Nelson L, Lassen MH, Fan E, Aras MA, Jordan C, Fleischmann KE, Melisko M, Qasim A, Shah SJ, Bajcsy R, Deo RC. Fully automated echocardiogram interpretation in clinical practice. *Circulation* 2018;138:1623–1635.